RESEARCH ARTICLE

American Journal of Botany

Botanical Society of America
leading scientists and educators since 1893

Reconstructing leaf area from fragments: testing three methods using a fossil paleogene species

Agathe Toumoulin[1,2,4], Lutz Kunzmann[1], Karolin Moraweck[1], and Lawren Sack[3]

Manuscript received 23 March 2020; revision accepted 9 September 2020.

[1] Senckenberg Natural History Collections Dresden, Königsbrücker Landstrasse 159, Dresden 01109, Germany

[2] Aix Marseille University, CNRS, IRD, INRA, Coll France, CEREGE, Technopole Arbois, 13545 Cedex 04, Aix-en-Provence BP80, France

[3] UCLA Ecology and Evolutionary Biology, 621 Charles E. Young Drive South, Box 951606, Los Angeles, CA 90095-1606, USA

[4] Author for correspondence (e-mail: agathe.toumoulin@gmail.com)

Citation: Toumoulin, A., L. Kunzmann, K. Moraweck, and L. Sack. 2020. Reconstructing leaf area from fragments: testing three methods using a fossil paleogene species. *American Journal of Botany* 107(12): 1786–1797.

doi:10.1002/ajb2.1574

PREMISE: Fossil leaf traits can enable reconstruction of ancient environments and climates. Among these, leaf size has been particularly studied because it reflects several climatic forcings (e.g., precipitation and surface temperature) and, potentially, environment characteristics (e.g., nutrient availability, local topography, and openness of vegetation). However, imperfect preservation and fragmentation can corrupt its utilization. We provide improved methodology to estimate leaf size from fossil fragments.

METHODS: We apply three methods: (1) visually reconstructing leaf area based on taxon-specific gross morphology; (2) estimating intact leaf area from vein density based on a vein scaling relationship; and (3) a novel complementary method, determining intact leaf length based on the tapering of the midvein in the fragment. We test the three methods for fossils of extinct *Eotrigonobalanus furcinervis* (Fagaceae) from two lignite horizons of the middle and late Eocene of central Germany respectively (~45/46 and 35/36 Ma).

RESULTS: The three methods, including the new one, yield consistent leaf size reconstructions. The vein scaling method showed a shift to larger leaf size, from the middle to the late Eocene.

CONCLUSIONS: These methods constitute a toolbox with different solutions to reconstruct leaf size from fossil fragments depending on fossil preservation. Fossil leaf size reconstruction has great potential to improve physiognomy-based paleoenvironmental reconstructions and the interpretation of the fossil record.

KEY WORDS ecophysiology; Europe; morphometrics; paleobotany; paleoclimate; plant taphonomy; swamp forests.

Fossil leaves can contribute importantly to the reconstruction of ancient environments. Indeed, some of their morpho-anatomical characteristics, the leaf traits, are particularly sensitive to plant growing environment (e.g., Royer, 2012; Roth-Nebelsick et al., 2017). Among leaf traits, leaf size is one of the most widely used characteristics (e.g., Bailey and Sinnott, 1915; Webb, 1959; Wolfe, 1979; Traiser et al., 2005; Peppe et al., 2011, 2018; Moraweck et al., 2019). However, consideration of leaf size is not always possible because of the frequently poor preservation of fossil specimens. A major concern is that not all categories of leaf sizes are equally preserved, which may induce a significant bias in the reconstruction of deep-time environmental and climatic parameters from the use of complete fossil leaves solely (see Hagen et al., 2019). Large leaves tend to be more fragile and are generally transported less far than small leaves, which bias the fossil record composition toward a too-high proportion of small leaves (e.g., Greenwood 1992; Hagen et al., 2019). Moreover, fragmentation of fossil leaves is a common sampling bias because laminae of larger leaves exceed the sizes of hand specimens and are thus often fragments, while smaller leaves better fit to hand specimen size and thus are often entirely preserved. For any quantitative reconstruction using leaf size and/or leaf-size derived parameters, e.g., leaf mass per area (Royer et al., 2007), the complete assemblage—including fragmented leaves—has to be taking into account, but it would require a reconstruction of the original leaf size from fragments. This study compares three methods to reconstruct the original area of fragmented fossil leaves.

Plant functional traits can be defined as "morpho-physiophenological traits, which impact fitness indirectly via their effects on growth, reproduction and survival, the three components of individual performance" (Violle et al., 2007). Leaf functional traits can indicate how plants respond to, or have adapted to, abiotic or biotic factors including temperature, drought, irradiance, and herbivory (e.g., Roth-Nebelsick et al., 2017 and citations therein). In case of fossil dicotyledonous leaves, functional traits include lamina size, lamina margin state

(toothed vs. untoothed), venation architecture, cuticle micromorphology, and quantitative parameters such as leaf mass per area (LM_A) and stomatal density and index (Moraweck et al., 2019). Inference based on functional traits of fossils must be thoughtful, especially with respect to the necessary assumption that traits reflect environmental and climatic conditions, ideally independently from their phylogenetic affiliation (Reich et al., 2003; Violle et al., 2007), and that the correspondence of traits and environment was the same in the past as in the present (Little et al., 2010). Furthermore, care must be taken to evaluate which functional traits can be reliably used to reconstruct specific paleoenvironmental variables such as mean annual precipitation (MAP) or mean annual temperature (MAT) (Hovenden and Van der Schoor, 2003; Little et al., 2010; Peppe et al., 2011). Notably, some leaf traits can also be affected by microclimatic factors and abiotic factors, such as the exposure of leaves to the sun, and differ strongly between sun and shade leaves on a single plant (e.g., Uhl and Mosbrugger, 1999; Crifò et al., 2014; Uhl, 2014; Wright et al., 2017). Two semiquantitative methods have been established: (1) the Leaf Margin Analysis (LMA), which correlates proportions of toothed and untoothed leaves of woody dicots in a fossil assemblage to MAT values provided by meteorological data of similar extant vegetation (Wilf, 1997; Uhl, 2006; see Royer et al., 2012); and (2) the Climate Leaf Analysis Multivariate Program (CLAMP, e.g., Wolfe, 1993; Wolfe and Spicer, 1999; Yang et al., 2011, 2015; http://clamp.ibcas.ac.cn), which correlates 31 leaf physiognomic characters with those of extant assemblages and then projects the climatic requirements of the physiognomically most similar extant data set to the fossil assemblage. For both methods, specific calibrations were introduced (e.g., Su et al., 2010 for LMA; Teodoridis et al., 2012 for CLAMP) because differences between regions could not be gathered in a single comprehensive equation. Application of these calibrations predicts climate based on the floristic similarity of the fossil assemblage to extant vegetation types.

Within these approaches, and separately, the use of leaf size (i.e., the area of the leaf lamina) to estimate environmental variables is extremely common. Many floristic comparisons across climatic gradients have illustrated the relationship between leaf size and multiple parameters such as MAP, MAT, nutrient availability, irradiance, and windspeed (e.g., Bailey and Sinnott, 1915; Webb, 1959; Wolfe, 1979; McDonald et al., 2003; Peppe et al., 2011; Tian et al., 2016; Wright et al., 2004, 2017). Smaller leaves are generally found in hot and dry localities (Wright et al., 2017), because small leaves have a thinner boundary layer that can enable close coupling with the air, as well as more rapid transpiration to prevent overheating above air temperature (Gates, 1965; Campbell and Norman, 1998; Uhl and Mosbrugger, 1999; Uhl et al., 2002; Okajima et al., 2012; Roth-Nebelsick et al., 2017). Smaller leaves also intrinsically have a higher vein length per area (i.e., "density") for large "major" veins, i.e., the midrib, secondary, and third-order veins (1°, 2°, and 3° veins, respectively), due to developmental scaling, because the 2° veins are generally patterned in the leaf primordium before the bulk of leaf expansion, which geometrically pushes these veins apart. Furthermore, in smaller leaves, the major veins may be narrower in diameter. These vein traits provide smaller leaves with drought tolerance (Scoffoni et al., 2011; Sack et al., 2012). However, at the global scale, leaf size is also positively correlated to MAT because large leaves are more vulnerable to chilling damage in cold climates (see also Peppe et al., 2011; Moles et al., 2014; Wright et al., 2017). Yet, large leaf sizes may be adaptive in moderately cold climates, where they are not subject to chilling. Indeed, large leaves have a better capacity to heat above-the-air temperatures such that the optimal leaf temperature for photosynthesis is reached, and water use efficiency is higher (Parkhurst and Loucks, 1972; Wright et al., 2017). Large leaves may also be adaptive if large leaves represent an economically effective means to achieve greater leaf area per plant mass. As for any other leaf trait used in paleoenvironmental reconstructions, leaf size use should be considered as one line of evidence to combine with other proxy data to provide robust reconstructions (Peppe et al., 2011).

While leaf size data for fossil assemblages is important for reconstruction of paleoenvironmental and/or paleoclimatic conditions, perfect data are scarce. Indeed, because of taphonomic processes and sampling biases, fossil leaves are often not completely preserved (Traiser et al., 2018). To make best use of fossil remains, procedures have been developed to estimate the intact leaf size from fragmentary leaf remains. Here, we test and refine three different approaches for the reconstruction of leaf sizes from fossil fragments: (1) visual estimation (VE) (Traiser et al., 2015, 2018), (2) vein scaling (VS) (Sack et al., 2012), and (3) a new method based on the midvein tapering (MVT).

As case study material for testing these methods, we use fossil leaves from the middle and the late Eocene. This material is of particular interest because it might display shifts coinciding with the strong global cooling that took place throughout the middle to late Eocene (e.g., Zachos et al., 2001, 2008; Mosbrugger et al., 2005; Westerhold et al., 2020). The fossil leaves are described as *Eotrigonobalanus furcinervis* (Rossmässler, 1840; Kvaček and Walther, 1989a), an extinct evergreen Fagaceae widely distributed in Eurasia and North America from the middle Eocene to the end of the Oligocene and constituting a dominant element of swamps and riparian communities during the middle and late Eocene (Mai and Walther, 2000; Winterscheid and Kvaček, 2016). Changes in leaf size may thus reflect climate changes, especially as the leaves are from a single long-lived species, and sampled from identical ecological and depositional settings in the same region. The material is almost exclusively fragmented to various degrees, hampering the direct application of most of the classical morphology and morphometry-based analyses (e.g., LMA; leaf size analysis for CLAMP; calculation of LM_A). We hypothesized that the intact leaf area could be reliably reconstructed from fragmented remains.

MATERIALS AND METHODS

Material, sites and selection of leaves

The *E. furcinervis* leaves used in this study were selected from paleobotanical collections based on their relative completeness and for representation of macromorphological variability (Fig. 1). These leaves come from two differently aged lignite seams in central Germany that were exposed in the opencast mines Schleenhain (SCHLE; Leipzig Embayment, former Weißelster Basin, n = 19 leaves) and Geiseltal (GTL; Geiseltal Basin, n = 37 leaves). SCHLE leaves exclusively come from a 15–20 cm thick layer in the upper part of the late Eocene main lignite seam complex of the Leipzig Embayment. They therefore represent a single taphocoenosis. They were collected between 1995 and 1997 in the Vereinigtes Schleenhain opencast mine. All SCHLE specimens are kept at the Senckenberg Natural History Collections Dresden, Dresden, Germany, Department *Museum of Mineralogy and Geology*, section Paleobotany (acronym MMG PB). For GTL, material from three close localities, i.e., mines Leonhardt, Otto, and Neumark-Süd, was combined for a representative sample

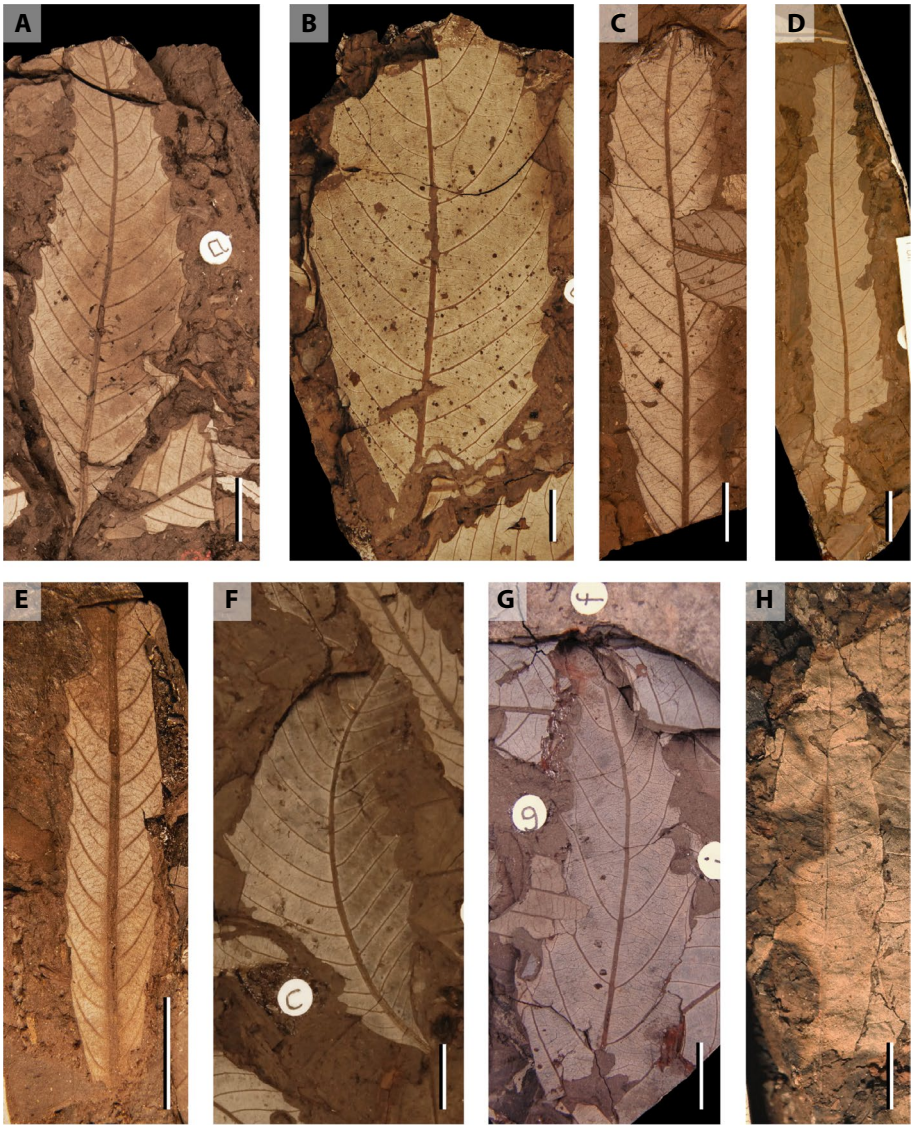

FIGURE 1. *Eotrigonobalanus furcinervis* leaf shape diversity. (A) MMG_PB_SchleEO_131-4; (B) MMG_PB_SchleEO_510-1-a; (C) MMG_PB_SchleEO_388-1-b; (D) MMG_PB_SchleEO_129-2-a; (E) MMG_PB_SchleEO_538-1-a; (F) MMG_PB_SchleEO_446-1-c; (G) MMG_PB_SchleEO_442-3-g; (H) MB.Pb._GTL-Pfä_38-a. Scale bar: 1 cm.

of *E. furcinervis* morphological variability in the older horizon. GTL leaves were originally collected during field missions in the 1950s to 1970s. They were excavated from several leaf litter beds in the middle part of the main Geiseltal lignite seam ("Mittelkohle" horizon). The GTL specimens are stored at the MMG PB for the site Leonhardt, and at the Museum of Natural History, Berlin, Germany, Leibniz Institute for Evolution and Biodiversity Science (acronym MB.Pb.) for the sites Otto and Neumark-Süd.

The two sites, approximately 20 km apart from each other, are located on former coastal-alluvial lowland plains at the southern margin of the Paleogene North Sea (Standke et al., 2008) (Fig. 2). Because of their paleogeographic position, the environment was strongly influenced by differently scaled transgression-regression phenomena. Lithostratigraphic sections contain interfingering strata of marine, brackish, lacustrine, and terrestrial siliciclastic sediments, illustrating repeated marine-terrestrial sediment cycles including paralic peat bog successions (Standke et al., 2008; Krutzsch, 2011). While SCHLE was directly located within a costal embayment, GTL was in a shallow depression in immediate coastal proximity. According to the regional palynological record (Krutzsch, 2011), the SCHLE leaf litter bed is accommodated in Spore-Pollen-Paleogene zone 18o, which is approximately 35–36 Ma in age (middle Priabonian, late Eocene; see Cohen et al., 2013) and the GTL leaf litter bed is from zone 15B, approximately 45–46 Ma (Lutetian, middle Eocene; see Cohen et al., 2013). The paleoenvironmental settings and depositional facies of both localities are almost identical except for the spatial extent of the peat bogs, which is a more local patch (extension about 15 × 5 km) in the case of GTL (Fig. 2). The paleovegetation of both sites represents the extratropical Atlantic Boreal phytoprovince (Mai, 1995), characterized by subtropical and humid climate in the middle to late Eocene (Moraweck et al., 2015). In general, alluvial landscapes are covered by midlatitudinal notophyllous evergreen broad-leaved riparian and swamp forests with few conifers and with palms (Mai and Walther, 2000; Kvaček, 2010). Preliminary studies have shown similarities among the floristic composition of GTL and SCHLE assemblages (Kunzmann et al., 2018). Both fossil assemblages are characterized by the predominance of *E. furcinervis* and contain additional leaf and carpological taxa that clearly assign them to predominantly azonal plant communities (i.e., Kvaček, 2010; Kunzmann et al., 2016), namely the "mixed Doliostrobus (and/or Quasisequoia) Fagaceae-Lauraceae forest" (Mai, 1995; Mai and Walther, 2000; Kunzmann et al., 2018). Thus, both leaf litter beds with mass occurrences of *E. furcinervis* represent similar palaeovegetation, i.e., coastal paralic lowland swamp forests, although of distinct geological ages (age difference of approximately 10 Ma). Both assemblages are considered being parautochthonous taphocoenoses, thus representing exclusively local vegetation (Kunzmann et al., 2018).

Previous taxonomic-systematic studies referred to a single fossil species *E. furcinervis* (Kvaček and Walther, 1989b; Kriegel, 2001), variable in lamina shape, lamina size, and margin morphology (Grímsson et al., 2016). Based on the predominance of distinct leaf morphotypes (i.e., leaf rough shape), Kvaček and Walther (1989b) described the fossil-formae *furcinervis*, *haselbachenses*, and *lyellii*. Forma *furcinervis*, mainly restricted to the Eocene, is characterized by conspicuously serrate margin and stellate trichomes along with simple and serial trichomes on the abaxial epidermis (Kvaček and Walther, 1989b). Formae *haselbachenses* and *lyellii* almost exclusively occur in the Oligocene and have almost entire-margined leaves or waved leaf margins, with rare or absent stellate trichomes on the lower epidermis for *haselbachenses*, and

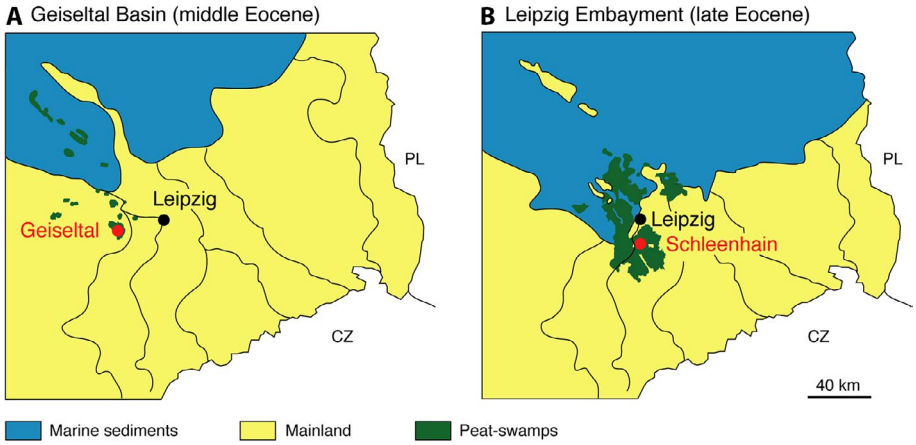

FIGURE 2. Site location maps: Geiseltal (GTL), and Schleenhain (SCHLE), after Standke et al. (2008). Marine sediments are in blue, terrestrial sediments in yellow, and peat-swamps in green. (A) The Geiseltal Basin (middle Eocene), containing the GTL sites. (B) Leipzig Embayment (late Eocene), containing the SCHLE site.

rare two-fingered trichomes for *lyellii* (Kvaček and Walther, 1989b). According to their gross morphology and cuticle micromorphology (cf. Kvaček and Walther, 1989a), the study material corresponds to *E. furcinervis* forma *furcinervis*. Henceforth, we refer to the species name *E. furcinervis*. Overall preservation of leaves varies between the two sites, such that it was not possible to use the same leaves for all analyses. At a glance, SCHLE leaves are better preserved than those from GTL. The 2° and 3° order veins are notably clearly visible in SCHLE leaves, whereas in GTL leaves, 2° veins are not always visible and 3° veins are not distinguishable. While SCHLE leaves could be identified solely based on their gross morphology (following Kvaček and Walther, 1989b; Kriegel, 2001) determination of GTL leaves were confirmed by leaf cuticle micromorphology, based on cuticle slides made using the procedure described by Kunzmann (2012) and identification was based on species characteristics described by Kvaček and Walther (1989b).

Methodologies for leaf size reconstruction

Three methods for reconstructing leaf size from fragments were applied comparatively, one of which is new. All analyses required high-resolution photographs with clear visibility of leaf architectural characteristics, notably the 1° and 2° veins. For this, each individual leaf was photographed (Nikon D5100, Nikon Corp., Tokyo, Japan) and scaled with ImageJ 1.48 (Schneider et al., 2012; National Institutes of Health, Bethesda, Maryland, USA), and their contrast and resolution were adjusted with Adobe Photoshop CS6 (Adobe, San Jose, California, USA) for greater visibility of leaf traits. The measurements carried out for the different methods are available in Appendix S1.

Leaf area reconstruction by visual estimation (VE)—The visual estimation method (VE) was originally made to create a database on Paleogene leaves and for statistical analyses of morphometric leaf traits (database Morphyll; Traiser et al., 2015, 2018; Roth-Nebelsick et al., 2017). This method requires the drawing of two different perimeters on each photo (Fig. 3). We used the open-source software Quantum-GIS, QGIS 2.18.3; http://qgis.org), and saved the outlines as shapefiles (.shp) from which quantitative information (e.g., length, width, surface) can be extracted with Structured Query Language (SQL) requests. The first perimeter corresponds to the actual outline of the leaf fragment (minimum outline, *LA_min*), enabling calculation of the specimen's preserved leaf area. The second perimeter is the visual estimation (maximum outline, *LA_VE*) representing the hypothesized original leaf before its fragmentation (Traiser et al., 2015). This method requires detailed knowledge on the leaf morphology of the taxon treated, including those of its feature variations. In estimating *LA_VE*, some characteristics such as the curviness of the margin and the diameter of the most apically preserved part of the midvein were considered. The leaf shapes resulting from *LA_VE* reconstruction were compared to *E. furcinervis* leaves from the MMG collections and to published descriptions (Kriegel, 2001; Knobloch et al., 1996; Rüffle et al., 1976). The ratio of *LA_min* to *LA_VE* gives an indication of the relative preservation of the specimen (Preservation Index: *PI*, ranging between 0 and 1.0; Roth-Nebelsick et al., 2017). Visual reconstructions with a *PI* value lower than 0.7 were considered unreliable (Traiser et al., 2015, 2018; Roth-Nebelsick et al., 2017).

Leaf length reconstruction based on Midvein Tapering (MVT)—The variability of *E. furcinervis* leaf shapes makes visual reconstructions challenging (Fig. 1). In particular, leaf length is highly variable in this fossil species, ranging from a few centimeters to more than 25 cm within a same fossil leaf assemblage (e.g., Hennig and Kunzmann, 2013). We propose a Midvein Tapering method (MVT) for estimating the original leaf length from leaf fragments based on the decrease of the midvein diameter from the leaf base to the apex and improving the reconstructions made with the VE method. The tapering of the midvein is calculated between two points of the fragmented leaf and allows estimation of the length of the missing part of the leaf (*AddL*). The MVT was applied to digitized leaves with a drawn *LA_min* perimeter, and the addition of estimated length of the missing apical section enables the drawing of a second reconstructed leaf lamina outline: *LA_MVT* (Fig. 3). The method is applicable to leaves with preserved bases. It requires three measurements per leaf (Fig. 3): two midvein diameters spaced within the leaf, (1) one close to the missing apical part (*MVDmin*), (2) one in the basal part, which should be wider (*MVDmax*), and (3) the distance in between the points of measurements of the two diameters (*dMVD*). The equation to estimate the missing part (*AddL*) is based on the Intercept theorem, and is constructed as follows:

$$AddL = \left(\frac{MVDmin}{MVDmax} \times dMVD\right) / \left(1 - \frac{MVDmin}{MVDmax}\right) \quad (1)$$

To assess the reliability of this method, we tested 30 complete leaves of extant *Formanodendron* (*Trigonobalanus*) *doichangensis*, a representative of the monophyletic trigonobalanoid clade of Fagaceae—considered as the most similar extant group of extinct *E. furcinervis* (Denk et al., 2012; Grímsson et al., 2016; Fig. 3). Herbarium material of MMG (n°5009) was collected from a native stand in western Yunnan, China by LK and KM in 2016. The

MVT method was applied to the fossil specimens that have preserved basal parts and a clearly visible midvein, enabling precise *MVDmin* and *MVDmax* measurements. Measured midvein lengths were compared to the lengths predicted by the formula in two ways, first by measuring *AddL* strictly following the midvein curviness, and second by drawing a straight line between *MVDmin* and an apical point centered between the margins.

Leaf area estimation based on vein scaling (VS)—Leaf size is negatively correlated across species with the density (i.e., length per leaf area) of major veins (1° to 3° veins), especially the 2° veins (Sack et al., 2012). The "leaf vein scaling" approach (VS; Sack et al., 2012), uses this negative scaling relationship to enable the estimation of the intact leaf area (i.e., leaf area before its fragmentation) from the vein density visible on a leaf fragment. This method was developed by Sack et al. (2012) on leaves from more than 400 extant species. It has thus far only been tested twice on fossil material and gave good results (Merkhofer et al., 2015; Hagen et al., 2019). However, the method has not been applied to determine size variation among leaves of a given species. This method was applied to specimens with well-preserved 2° veins (SCHLE: n = 19; GTL: n = 37). Vein density can be represented by (1) its inverse proxy, i.e., the interveinal distance, or (2) directly measured as the vein length within a given area (in millimeters per square millimeters [mm/mm^2]), which has been described as more accurate (Uhl and Mosbrugger, 1999). The 2° veins were identified according to Ellis et al. (2009). Vein density was measured in two ways. First, following the protocols of Sack et al. (2012) and Merkhofer et al. (2015), including intersecondary veins (also known as minor 2° veins) when they were present (Ellis et al., 2009). Second, 2° vein density was measured without taking intersecondary veins into account. Although considered as minor 2° veins, intersecondary veins develop after the larger 2° veins, and

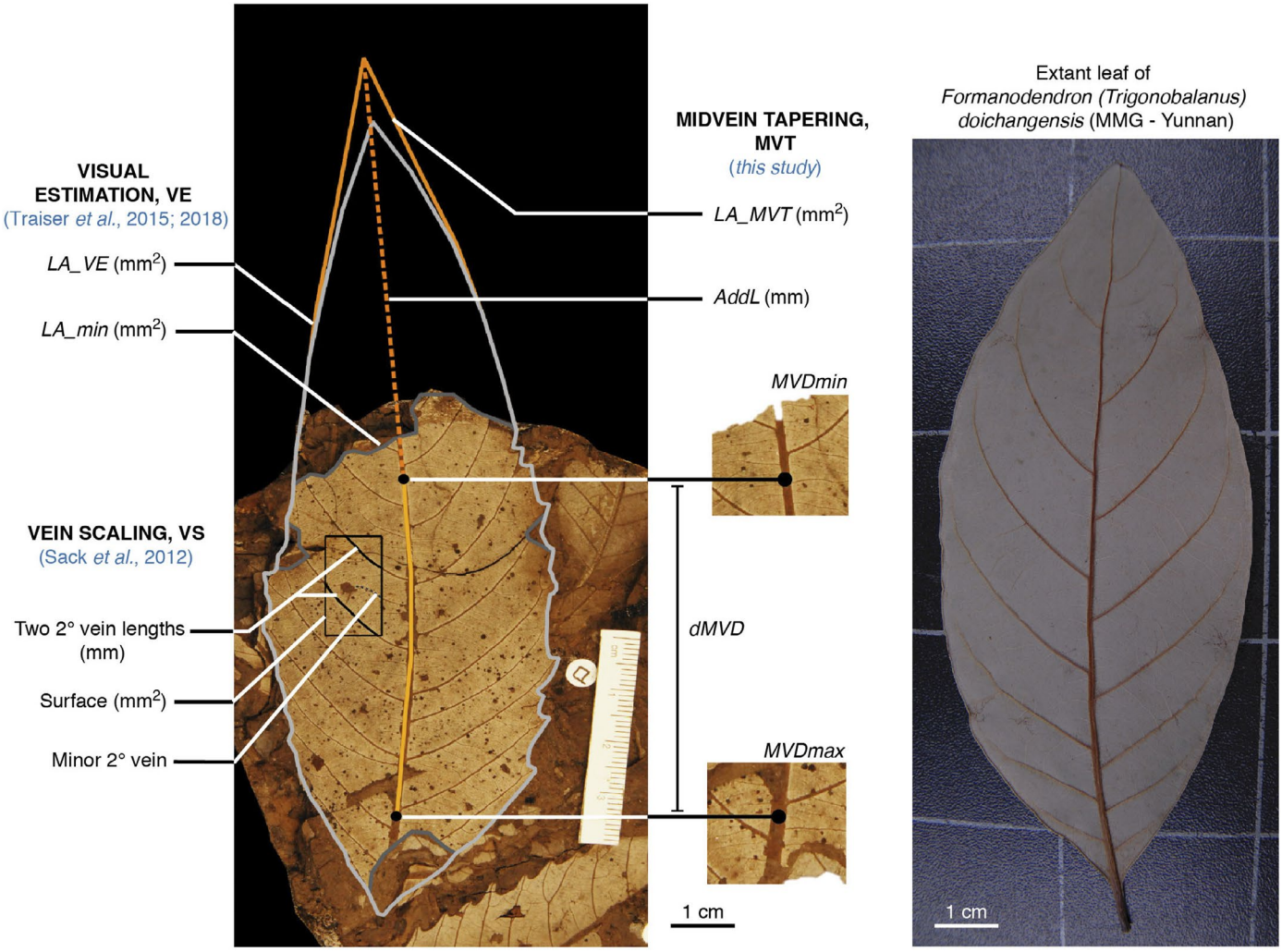

FIGURE 3. Measurements for the different leaf area reconstruction methods. *Visual estimation reconstruction, VE* (cf. Morphyll database, Traiser et al., 2015, 2018): *LA_min* = the fossil leaf outline; *LA_VE* = the putative outline of the leaf before its fragmentation. *Midvein tapering method, MVT* (this study): *MVDmin* / *MVDmax* = two points of diameter of the 1° vein diameter measurement (*MVDmin* < *MVDmax*), *dMVD* = length of the 1° vein between the points *MVDmin* and *MVDmax*; AddL = additional/missing length; *LA_MVT* = the possible outline of the leaf before its fragmentation according to *AddL*. *Vein scaling, VS* (cf. Sack et al., 2012): the length of two 2° veins within a rectangle and the area of this rectangle. *Eotrigonobalanus furcinervis* fossil leaf (left): MMG_PB_SchleEO_510-1-a. MVT method was tested on 30 leaves of extant *Formanodendron* (*Trigonobalanus*) *doichangensis* (Herbarium material of MMG, n°5009; collected by LK and KM from native stand in SW China).

thus show different developmental scaling. In addition, they are not present on all our leaves. As proposed by Sack et al. (2012), two vein lengths were measured within rectangles oriented parallel to the primary vein in the assumed middle part of the lamina. These rectangles were 0.4 cm^2 on average, and if possible, two measurements per leaf were made. The formula presented in the original publication (Sack et al., 2012) enables estimation of leaf area from the intercept (a) and slope (b) of the linear relationship between log-transformed data for leaf area and 2° vein density ($V2D$):

$$log10\,(leaf\,area) = a + b \times log10\,(subsample\,2^\circ\ vein\,density) \quad (2)$$

We first applied (1) the trend provided by Sack et al. 2012 that was derived from a global modern set of species for vein scaling with leaf size, $a = 1.96$ and $b = -0.04$ ($R^2 = 0.80$, $P < 0.001$, $n = 386$), to reconstruct intact leaf sizes of GTL and SCHLE fossil leaf fragments; these reconstructions are referred to as "*LA_Sack*". We also fitted additional linear regressions on distinct subsamples of the original data set of Sack et al. (2012) for greater correspondence to the gross morphology of *E. furcinervis* (Fig. 4). These additional calibration linear models were (2) exclusively pinnately-veined leaves, excluding *Calophyllum longifolium* (a species with distinctive veins that does not follow the global scaling trends; Sack et al., 2012) (model: "*Cal_Pin*", $n = 392$); (3) only pinnately veined leaves from Fagales (model: "*Cal_Fgl*", $n = 67$); (4) only pinnately veined leaves from Fagaceae (model: "*Cal_Fgc*", $n = 53$); and (5) using the most complete *E. furcinervis* fossil leaves from the present study (model: "*Cal_Eo*", $n = 33$). Calculations made from this last subsample were made based on *V2D*s and *LA_VE* of leaves with *PI* > 70%, either taking minor 2° veins into account for the calculation of vein density ("*Cal_Eo_inter*") or not ("*Cal_Eo_nointer*") (Fig. 4D, E). All slopes and intercepts of these linear regressions are shown in Fig. 4. These regressions were applied to *E. furcinervis V2D* measurements (n *V2D* measurements = 94) to obtain leaf area estimations (Appendix S1). When two density measurements were possible on a leaf, their size reconstructions were averaged to have one value per leaf (n leaves = 56).

Finally, since the real intact sizes of the leaves before their fragmentation are unknown, the leaf sizes reconstructed with the VS method were tested against the leaf fragment area, *LA_min*, which is the only assured size quantification. The comparison of VS estimates and *LA_min* highlight the number of aberrant reconstructions, i.e., where intact leaf size was predicted as being smaller than the fragment size for a given leaf. It is a minimal error because to a lesser extent, the original size could also be underestimated without being less than the size of the fossil fragment. The percentage of these aberrant estimations was calculated for each model and noted as "*ERRORmin*".

Statistical analysis—We assessed the leaf-trait variation within and between our study sites, and compared the different methods, using Rstudio v.1.0.136 (RStudio Team, 2016). Shapiro-Wilk and Fisher tests were used to evaluate the data distribution normality and the variance homogeneity. The comparison of quantitative values of a given variable (e.g., *LA_VE* SCHLE vs. *LA_VE* GTL) were made with a Student's t-test when the data followed a normal distribution and had equal variances, or otherwise, a Mann-Whitney test. Correlations between quantitative variables were made with Pearson tests when the data followed a normal distribution and with equal variances, and otherwise Spearman tests. Finally, a Kruskal-Wallis test was

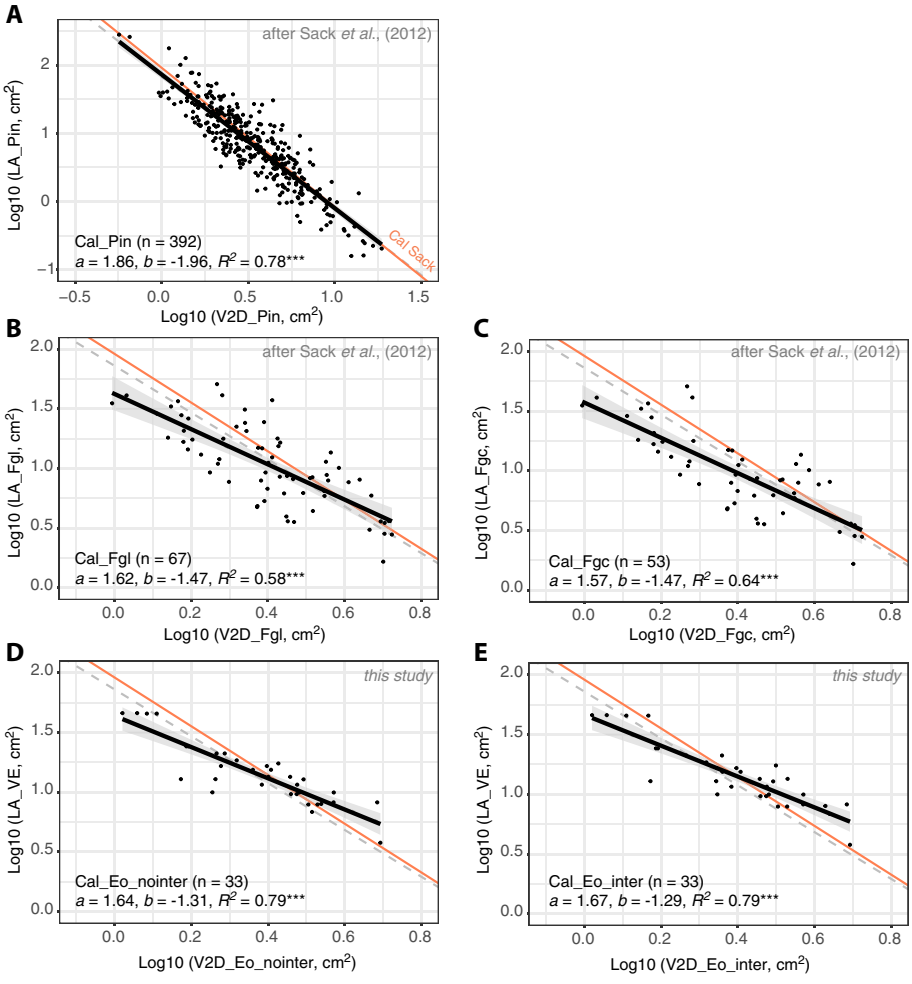

FIGURE 4. Vein scaling method (VS): relationship between leaf area and 2° vein density (*V2D*) as calculated from different data sets. (A–C) are subsets from Sack et al. (2012) global data set with (A) pinnate leaves only, (B) Fagales leaves, (C) Fagaceae leaves. (D–E) show leaf area and *V2D* relationship from *E. furcinervis* best preserved leaves (*PI* > 0.70). For these two calibrations, leaf size comes from *LA_VE*, which is assumed to be of good quality because the leaves are well preserved. For (D), *V2D* was measured without inclusion of minor 2° veins (*"Cal_Eo_nointer"*), while (E) includes these veins ("*Cal_Eo_inter*"). For all regressions, a is the intercept; b is the slope; r^2 is the coefficient of determination; p*** indicates p-values < 0.001 and the statistical significance of the regression. Coral line is the best-fitting relationship given by Sack et al. (2012), where $a = 1.96$ and $b = -2.04$, with $r^2 = 0.8$ and $p < 0.001$. Dashed grey line is the regression line from (A).

conducted to compare the different methods. Unilateral statistics were favored (i.e., when the sample average values gave expectations about the difference direction, e.g., GTL leaf sizes < SCHLE leaf sizes.

RESULTS

Sample description

Considering all the *E. furcinervis* leaves available in the MMG PB collection (*n* leaves > 500), and the measurements of leaves with ≥70% preserved lamina, leaf shape is simple, ovate or elliptic, with a length approximately ranging between 4.9 and 20.2 cm (mean: 12.5, s.d. = 3.8), and a length/width ratio of 2.6–10.1 (mean = 5.6, s.d. = 1.9), acute apical and basal outline angles, and an elongated petiole. The major vein architecture is pinnate with craspedodromous secondary veins. The teeth are acute, of irregular size and distribution is along the lamina margin. Eight leaf morphotypes were identified in the collection (Fig. 1), with similar representatives in the SCHLE and GTL assemblages, except for one type (Fig. 1H), which only occurs among GTL leaves. The average leaf sizes calculated per site using the visual reconstructions (VE), the midvein tapering (MVT) and vein scaling (VS) are given in Table 1.

Leaf area reconstruction

The VE reconstructions resulted in estimates of lamina area of 3.8–46.0 cm² (mean = 15.5, s.d. = 9.2, *n* = 56 leaves). According to this reconstruction, GTL leaves were not significantly smaller or larger than SCHLE leaves (Mann-Whitney test: W = 430, $P = 0.08$) although mean values point toward larger leaves for SCHLE.

The use of midvein tapering to estimate leaf length was supported by the analysis of extant *Formanodendron* (*Trigonobalanus*) *doichangensis* leaves. The measured apical leaf length (located apically of *MVDmin*) was statistically similar to the estimated *AddL* (Mann-Whitney test: $W = 437$, $P = 0.58$) and the two were positively correlated (Spearman test: $\rho = 0.64$, $S = 1600.7$, $P < 0.001$). No statistical difference was found whether measuring the apical length by drawing a straight line or by following the natural leaf midvein curve (Student's t-test: $t = 0.06$, df = 58, $P = 0.96$). Because the midveins of GTL fossil leaves were badly defined or preserved, the *MVT* method was only applied to SCHLE fossil leaves (*n* = 19 leaves); the average estimated leaf size was 20.5 cm² (s.d. = 12.6).

The negative relationship of secondary vein density with leaf size was significant within all the tested regression calibration data sets (*Cal_Sack*, *Cal_pin*, *Cal_Fgl*, *Cal_Fgc*, *Cal_Eo_nointer, Cal_Eo_inter*) ($P < 0.05$), with coefficient of determination (R^2) varying from 58% (*Cal_Fgl*) to 80% (*Cal_Sack*; Sack et al., 2012) (Fig. 4). However, a substantial proportion of aberrant leaf size reconstructions, *ERRORmin* (i.e., the percentage of reconstruction where intact leaves were predicted as smaller than the fossil fragment, *LA_min*) occurred, depending on the calibration data set used and whether or not minor 2° veins are taken into account (Table 1, Fig. 5). This frequent underestimation were observed within every leaf morphotype (Fig. 1), but, because of the low number of specimens, it was not possible to find a relationship between these errors and leaf types. On the one hand, the lowest *ERRORmin* was found for *LA_Eo*, which was based on the fossil leaves of *E. furcinervis*. When calibration data sets were based on other species, *ERRORmin* increased with the specificity of the data set, i.e., $ERRORmin_{(LA\_pin)} < ERRORmin_{(LA\_FGL)} < ERRORmin_{(LA\_FGC)}$ (Table 1). On the other hand, as a result of the negative relationship between leaf size and vein density, the number of these underestimations increases when the intersecondary veins are used in addition to major 2° veins to calculate the vein density for all calibration data sets except for *LA_Eo* (Table 1, Fig. 5). *ERRORmin* is, for instance, 12.5% higher in *LA_Sack* with intersecondary veins.

Based on (1) the strength of the relationship of secondary vein density with leaf size (R^2, Table 1), and (2) the proportion of aberrant leaf size reconstructions (*ERRORmin*, Table 1), it is possible to select the most adequate regression for estimating *E. furcinervis* intact leaf sizes from the 2° vein density measurements. With the second highest R^2 and the lowest *ERRORmin*, the species-specific data, *LA_Eo*, appeared to be the most effective calibration to calculate *E. furcinervis* leaf size.

Methods comparison

All methods gave similar estimation of leaf size for SCHLE (Kruskall-Wallis test: $\chi^2 = 1.248$, df = 3, $P = 0.74$) (Fig. 6.A). A close

TABLE 1. Leaf area reconstruction and size difference between Schleenhain (SCHLE) and Geiseltal (GTL) leaves.

	LA_VE	LA_MVT	LA_Sack	LA_Pin	LA_Fgl	LA_Fgc	LA_Eo_nointer	LA_Eo_inter
All data	15.5 cm² (sd 9.2)	na	14.1 cm² (sd 12.9)	11.9 cm² (sd 10.3)	10.3 cm² (sd 6.2)	9.1 cm² (sd 5.5)	12.3 cm² (sd 6.4)	12.4 cm² (sd 6.5)
SCHLE	18.2 cm² (sd 11.4)	20.5 cm² (sd 12.6)	22.6 cm² (sd 18.3)	18.8 cm² (sd 14.6)	14.6 cm² (sd 8.3)	12.8 cm² (sd 7.3)	16.8 cm² (sd 8.4)	16.6 cm² (sd 8.8)
GTL	14.2 cm² (sd 7.7)	na	9.7 cm² (sd 5.3)	8.3 cm² (sd 4.4)	8.1 cm² (sd 3.2)	7.1 cm² (sd 2.8)	10.0 cm² (sd 3.5)	10.0 cm² (sd 3.4)
ERROR*min* (minor V2)	0 %	0 %	32.1 %	37.5 %	44.6 %	58.9 %	na	10.7 %
ERRORmin (no minor V2)	0 %	0 %	19.6 %	28.6 %	37.5 %	53.6 %	10.7 %	na
Size difference	No $P = 0.09$ W = 430	na	Yes $P < 0.01$, W = 552					Yes $P < 0.01$ W = 545

Notes: Leaf area estimations are given for the different methods: visual estimation, VE (*LA_VE*), midvein tapering, MVT (*LA_MVT*) and vein scaling, VS (*LA_Sack, LA_Pin, LA_Fgl, LA_Fgc, LA_Eo_nointer, LA_Eo_inter)* using regressions based on different calibration data sets (Fig. 4). VS size estimations given in this table were made without taking intersecondary veins into account in the measurements of vein density, except for *LA_Eo_inter*. *ERRORmin* is the percentage of leaf size reconstructions with smaller sizes than the measured fossil leaf fragment (*LA_min*). Because leaf size reconstruction with the VS method were conducted both with and without considering minor 2° veins length in 2° vein density, this parameter is given twice per the calibration data set. The significance of the difference between SCHLE and GTL leaf sizes are given by Mann-Whitney-Wilcoxon test *P*-values. $P < 0.05$ indicates significant difference in leaf size between GTL and SCHLE. Nonavailable values are noted: "na".

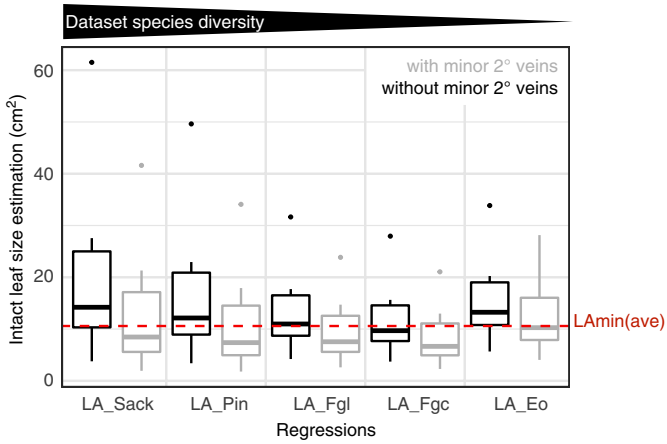

FIGURE 5. Leaf size reconstructions with the different calibration of the vein scaling method (VS). *LAmin(ave)* line shows the average *LA_min* value for this leaf assemblage. This figure uses the 19 leaves (10 from SCHLE, 9 from GTL), which enabled the measurement of *V2D* with intersecondary veins. Size estimations for all leaves of SCHLE and GTL are visible in Fig. 6.

correspondence was observed between the VE reconstructions and estimations using either the MVT (*LA_MVT*) or the VS (*LA_Sack* and *LA_Eo_nointer*) methods (Fig. 6B). Leaf length estimation using the MVT method (*LA_MVT*) provided values closest to VE reconstructions (*LA_VE*) even though slightly larger leaves are almost systematically predicted. Leaf area reconstructions based on the VS method (*LA_Sack* and *LA_Eo_nointer*) were consistent with the other methods but tended to over- or underestimate the size of largest leaves depending on the calibration used (Fig. 6B). Each of the VS calibrations indicated significantly smaller leaves in GTL than in SCHLE (Mann-Whitney test: $W = 552$, $P < 0.01$, see Table 1), a difference not resolved by the visual estimations (*LA_VE*; Mann-Whitney test: $W = 430$, $P = 0.09$). Depending on the calibration used, this leaf size increase from the middle to late Eocene ranges from 57.0% (*La_Sack*) to 40% (*LA_Eo_nointer*). The comparison of methods that could be applied on GTL leaves (VE and VS) however yield different results (Kruskal-Wallis test: $\chi^2 = 12.381$, df = 2, $P = < 0.01$).

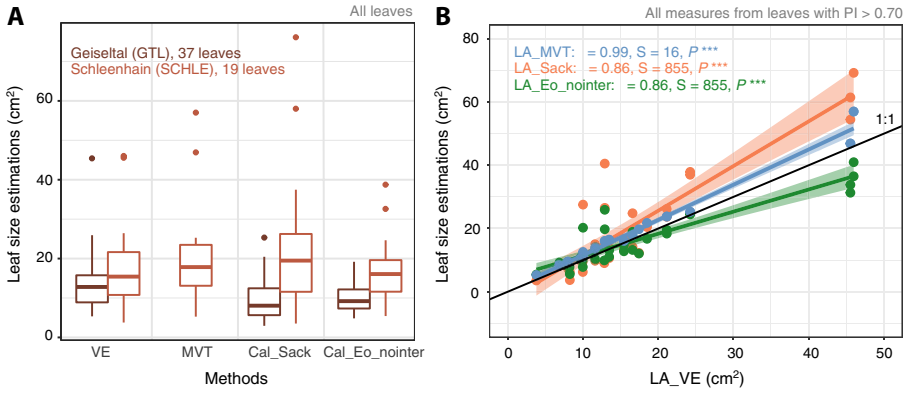

FIGURE 6. Comparison of different leaf size reconstruction methods. (A) Boxplot of leaf size reconstructions using visual estimation (VE), midvein tapering (MVT), vein scaling (VS) using the Sack et al., 2012 calibration (*Cal_Sack*) and *Eotrigonobalanus furcinervis* calibration without intersecondary veins (*Cal_Eo_nointer*). (B) Comparison of the different leaf size reconstructions to VE leaf reconstructions (LA_VE). For (B), only leaves with a *PI* > 0.7 are used because MVT could not be applied on GTL leaves. Values given in (B) are results of the Spearman rank correlation test, where ρ is the correlation coefficient, *S* the value of the statistic, and *P**** indicates *p*-values < 0.001 and thus the statistical significance of the regression. Size estimations from vein scaling (*LA_Sack* and *LA_Eo_nointer*) shown in this figure were made without taking intersecondary veins into account in the measurements of 2° vein density (*V2D*). The black line is the 1:1 line.

DISCUSSION

Methods for leaf area reconstruction

Overall, all leaf size reconstruction approaches tested could be applied reliably to fragments. The leaf size reconstructions were similar across the three methods for SCHLE but not to less-well preserved GTL leaves (VE and VS reconstructions, Table 1). This suggests that these methods are good leaf size reconstruction tools but they should be selected depending on the leaf lamina completeness and the preservation of major veins. In the next section, we discuss the limitations of each of these methods and compare them with each other.

The leaf sizes obtained with VE (*LA_VE*) showed no significant difference between GTL and SCHLE leaves, whereas a shift to smaller leaves was observed with the VS method. Although VE reconstructions can be used to estimate leaf size, the approach is subjective and potentially unreliable especially in highly fragmented leaves. While advanced knowledge of leaf morphology may improve this method, for taxa with extremely variable morphological features, such as *E. furcinervis* (Kriegel, 2001), this approach is stretched to its limits. This bias seems to be particularly strong for GTL leaf reconstructions, which had a larger leaf size with the VE approach compared to other methods (Table 1). For these leaves, *LA_VE* was probably overestimated because of a too-coarse preservation of leaf characteristics. Because *LA_VE* could have been misestimated, we cannot refer to a PI beyond which, using the VE method would not be appropriate. Furthermore, the quality of reconstructions with this method is also strongly dependent on leaf shape and its variability (i.e., leaves with low intraspecific variability are easier to reconstruct). However, taking into account the size of a leaf as estimated with the VS method, we can recalculate another preservation index (*PI2* = *LA_Eo_nointer*/*LA_min* *100). With this indicator, SCHLE leaves have a *PI2* = 0.80, while for GTL leaves *PI2* = 0.67. If the estimates made with the VS method are meaningful, it can be assumed that a PI for fragmented *E. furcinervis* leaves of 67% is already insufficient to allow reliable reconstructions with the VE method.

The MVT method introduced in this study was reliable when tested on leaves of the extant species *Formanodendron (Trigonobalanus) doichangensis* (cf. Section Results, Leaf area reconstruction, Spearman test: $\rho = 0.64$, $S = 1600.7$, $P < 0.001$). The proximity between additional lengths measured

linearly, or accounting for the curve of its margin, indicated that extrapolating a straight line was adequate for leaf length reconstruction in this species, which has moderate midvein curvature. *Formanodendron (Trigonobalanus) doichangensis* is only one extant species within the trigonobalanoid clade that we have treated. The species was chosen based on material availability and the controlled sampling strategy, which was getting leaves from a single tree in its native stand and vegetation type covering as much as possible the gross-morphological variability of the species. Therefore, the sampling of these leaves was made with respect to the variability of leaf traits that might be expected in a fossil assemblage. Such a sampling strategy is not a primary goal for collecting herbarium specimens, which is why it is not often found for herbarium specimens. Additional extant taxa closely related to *E. furcinervis* should be tested in the future.

The leaf area for SCHLE reconstructed with the MVT method matched well with other estimations (VE and VS). However, the MVT could not be applied to GTL leaves, because of inappropriate preservation of midveins. This method is likely applicable for many taxa, because universally the midvein diameter decreases acropetally in angiosperm leaves (Sack and Scoffoni, 2013). The MVT method proposed here is based on the assumption that this decrease is linear through the leaf. However, the decrease of leaf vein diameter depends on the number of other higher order veins that branch out (Price et al., 2013). Thus, the method could be improved by knowing (1) the number of 2° veins for a given taxon, and (2) its average distribution (*V2D*) through the leaf; this information may be used to derive a coefficient to adjust the length of the missing part of a fossil leaf. This method should be further tested on material of other extant species paying attention to specific, phenological, and environmental diversity, including leaves of different shapes (e.g., ovate, obovate, elliptic).

When applying VS method to reconstruct leaf area, the best estimation was found when using equations based on *E. furcinervis* (*LA_Eo*). The cross-species global regression presented by Sack et al. (2012; here *LA_Sack*) was not the most appropriate for estimating leaf area variation across *E. furcinervis* leaves, even though that formula was usefully applied across an assemblage of fossil fragments of multiple species (Merkhofer et al., 2015; Hagen et al., 2019). Even though the vein scaling with leaf size was strong within a given taxon as has been reported across taxa, and the cross-species relationship can be used to predict intact leaf size, the relationship of leaf size to 2° vein density shows a specific scaling within a given species, providing greater accuracy in leaf size reconstruction for that species. Thus, for sets of monospecific specimens such as those treated in the present study, developing a calibration from the best-preserved specimens, like *Cal_Eo*, seems to be a more efficient alternative solution. In addition, our measurements performed on intersecondary veins show a strong tendency to underestimate the size of the leaves when they are taken into account. Unless this type of vein is present on all the leaves studied and a specific calibration of leaf size and secondary vein density is performed, we do not recommend the measurement of these veins.

The different methods tested in this study and their intercomparison enable the following analyses to be prescribed. On well-preserved material, both VE and VS methods are recommendable because they provide meaningful results. For relatively well-preserved assemblages, whose leaf morphologies are known and variabilities are well-structured, the VE method seems to be the most suitable: it is simple and allows a visual check on the reconstructed leaf surface compared to other completely preserved leaves of the same taxon. The VS method is nevertheless to be preferred in the following cases: (1) incomplete leaves whose manual reconstructions would be biased, i.e., by a hardly ascertainable morphological variability, and (2) leaves belonging to unidentified specimens with unknown plasticity of leaf morphology. This method has the advantage of allowing individuals who are not specialists in the morphology of the fossil taxa to reconstruct leaf sizes for using them as paleoenvironmental proxy. Finally, the first tests carried out on the MVT method that we propose in this study seem promising, but these analyses do not enable us to know its applicability or limitations. Its use on a larger number and type of leaves will provide more information on its application in a specific context.

Application to paleoenvironmental reconstructions

The floristic composition of the fossil plant communities (and thus forest structure) are almost identical as far as it can be assumed from paleobotanical and taphonomic data (see Materials and Methods section of this article; Kunzmann et al., 2018). Indeed, both sites correspond to similar environmental settings (coastal lowland swamps) with mixed broadleaved-conifer lignite swamps forests. Because of specific environmental characteristics, low nutrient availability, and water-saturated soil, such forests are generally less diverse than other zonal or azonal vegetation units, with only medium-sized trees (the settlement of heavy trees is limited by the soil softness). Moreover, taphonomic conditions for the origin of both leaf assemblages are also identical. Leaf litter beds in lignites are usually accumulated in ponds or pools within the peat bog being derived from the plants in immediate proximity of the water body. This causes parautochthonous phytotaphocoenosis (e.g., Kunzmann, 2012; Kunzmann et al., 2018). Therefore, the differences resolved in leaf size between the sample assemblages of the two sites using vein scaling analysis of leaf fragments may reflect adaptations to local-to-regional climatic conditions or differences in habitat conditions, which could not be traced so far. Leaf traits are shaped by the combination and interaction of many environmental and climate parameters that are difficult to disentangle (Little et al., 2010; Peppe et al., 2011; Wright et al., 2017), and thus, for paleoenvironmental inference, differences in leaf area should be combined with other information of morphology and paleoecology (Peppe et al., 2011). Furthermore, while *E. furcinervis* was a dominant species, it was native to an unusual habitat, i.e., a long-term wide-ranging coastal mire, which might represent a highly local environment. Despite this, given the significance of leaf size increase between GTL and SCHLE, we briefly consider potential environmental drivers of this trend.

Major environmental drivers of leaf size globally and historically are soil and/or atmospheric moisture. However, both sites were humid environments, similar to the modern landscape of the Everglades (Florida, USA), and former paleobotanical studies did not reconstruct significant changes in MAP between the middle and late Eocene of this area (Mosbrugger et al., 2005; Kvaček et al., 2014; Moraweck et al., 2015). Thus, even assuming changes in the hydrological cycle associated with reductions in the partial pressure of carbon dioxide (pCO_2), humidity was not likely a limitation on vegetation function or a factor in constraining leaf size in GTL nor in SCHLE (Traiser et al., 2005; Wright et al., 2017).

Another major driver of leaf size shifts globally is temperature. However, relating the leaf size increase observed between GTL and SCHLE leaves to this parameter is not straightforward and is debatable. First, although the marine record describes the Eocene cooling initiation right after the Early Eocene Climatic Optimum (~50 Ma; Zachos et al., 2001, 2008), the Central Europe vegetation reflects moderate changes in MAT in this area from the late-middle to the late Eocene (Kvaček et al., 2014; Moraweck et al., 2015; Kunzmann et al., 2016). On the one hand, a recent meta-analysis of the geographical distribution of current vegetation leaf size has shown a positive correlation between leaf size and temperature (Wright et al., 2017). In the event of a pronounced cooling in this area and its record by the vegetation, we may have expected a decrease in leaf area instead of its increase, as observed for *E. furcinervis*. On the other hand, for climatic temperatures that are not extreme, i.e., above the threshold for chilling damage, and below the threshold for overheating damage, leaf energy balance models show that larger leaves would tend to be adaptive in colder climates, achieving higher leaf temperatures, photosynthetic rates, and water use efficiency (Parkhurst and Loucks, 1972; Okajima et al., 2012). According to this second hypothesis, increased leaf size might be consistent with a moderate cooling. Alternatively, a strengthening of temperature seasonality (i.e., mean annual range of temperatures), with colder winters, has been documented in Europe from the late-middle Eocene to the early Oligocene (e.g., Mosbrugger et al., 2005; Eldrett et al., 2009; Hren et al., 2013; Tanrattana et al., 2020). Among different temperature metrics, leaf size seems particularly correlated to temperature of the growing season (Wright et al., 2017). We may hypothesize that such change of the annual distribution of temperatures could have had an effect on plant growing season length and thus leaf physiognomy. However, a relationship between leaf size and seasonality remains to be demonstrated.

Other climatic and environmental parameters, which are sometimes hard to reconstruct in deep-time environments, may also have had an effect on leaf size. For instance, wind speed and cloud cover directly affect leaf temperature and the quantity of light perceived. Furthermore, different paleoenvironmental characteristics may have more of an effect on specific values of leaf traits than global climate, e.g., canopy openness or soil nutrient availability. Finally, because leaf size is linked to many species response to their environments, one cannot exclude possible evolutionary effect. Thus, given our knowledge on Central Europe paleoenvironments, the increase in leaf size between GTL and SCHLE middle and late Eocene fossils could be related to different parameters. Further analysis of other plant functional traits and of the paleoecology of these coastal mires may provide further clues toward interpretation of this pattern.

CONCLUSIONS

The fragmentation of leaves is a commonly encountered problem in the fossil record and the use of fossil leaf assemblages for paleoenvironmental and paleoclimatic reconstructions requires suitable tools for the reconstruction of original leaf laminae. Leaf size and other morphometric parameters and estimates, such as leaf mass per area, are important proxies for reconstructing plant functional ecology, climate, and habitat information. Our analysis showed that three methods to estimate the original leaf size from fossil leaf fragments were effective for the fossil species *E. furcinervis* from two distinctly aged leaf litter beds. The visual estimation approach (VE), the vein scaling method (VS), and a newly introduced third method, the midvein tapering approach (MVT) all provided consistent estimates. These approaches present a toolbox for estimating intact leaf size from fossil fragments with different solutions according to the context, i.e., degree of fragmentation, intraspecific morphological variability, and visibility of venation. In the case of relatively well-preserved leaves of species for which knowledge of the lamina shape exists, and especially for taxa with low intraspecific variability, the VE method appears particularly valuable. Conversely, MVT and VS, being less prone to the processor's subjectivity, should be favored for markedly fragmented leaves or for species with conspicuous morphological variability in leaf architecture. The MVT method appears promising especially for poorly preserved fossils, having only their basal parts and midveins preserved, for which other methods are not applicable. In all cases, studies in parallel of extant species related to the fossils under investigation provide improved calibrations for leaf size reconstruction, and also can provide information on the mechanisms shaping physiognomic diversity and the correspondence of environmental factors with leaf traits.

ACKNOWLEDGMENTS

The authors thank the University of Montpellier (France) and the "Occitanie" region for funding A. Toumoulin's work visit in Dresden; to Carola Kunzmann and Dorothea Bräutigam (both MMG Dresden) for their careful preparation of the collection material; the paleobotanical curators Stephan Schultka and Barbara Mohr at the Museum of Natural History Berlin, Leibniz Institution for Biodiversity Research; and Antoine Champreux and Pierre Ganault for helpful discussions on the methodology. Finally, the authors sincerely thank an anonymous associated editor, and reviewers Thomas Denk and Daniel Peppe for their constructive feedback, which greatly improved the manuscript. We acknowledge use of RStudio (https://rstudio.com/) for statistical analysis in this paper.

AUTHOR CONTRIBUTIONS

A.T. performed the measurements, analysis, drafted the manuscript and designed the figures. L.K. supervised the work. L.S. helped in applying the vein scaling method. L.K., K.M., and L.S. aided in interpreting the results. All authors discussed the results and commented on the manuscript.

DATA AVAILABILITY

All measurements are available as tables in the Supporting Information section.

SUPPORTING INFORMATION

Additional Supporting Information may be found online in the supporting information tab for this article.

APPENDIX S1. Leaf traits and size measurements used in this study.

LITERATURE CITED

Bailey, I. W., and E. W. Sinnott. 1915. A Botanical Index of Cretaceous and Tertiary Climates. *Science* 41: 831–834.

Campbell, G. S., and J. M. Norman. 1998. An Introduction to Environmental Biophysics, Springer, New York.

Cohen, K. M., S. C. Finney, P. L. Gibbard, and J.-X. Fan. (2013; updated). The ICS International Chronostratigraphic Chart. *Episodes* 36: 199–204.

Crifò, C., E. D. Currano, A. Baresch, and C. Jaramillo. 2014. Variations in angiosperm leaf vein density have implications for interpreting lie form in the fossil record. *Geology* 42: 919–922.

Denk, T., F. Grímsson, and R. Zetter. 2012. Fagaceae from the early Oligocene of Central Europe: persisting new world and emerging old world biogeographic links. *Review of Palaeobotany and Palynology* 169: 7–20.

Eldrett, J. S., D. R. Greenwood, I. C. Harding, and M. Huber. 2009. Increased seasonality through the Eocene to Oligocene transition in northern high latitudes. *Nature* 459: 969.

Ellis, B., D. C. Daly, L. J. Hickey, and J. D. Mitchell. 2009. Manual of Leaf Architecture. Comstock Publishing Associates, New York.

Gates, D. M. 1965. Energy, Plants, and Ecology. *Ecology* 46: 1–13.

Greenwood, D. R. 1992. Taphonomic constraints on foliar physiognomie interpretations of Late Cretaceous and tertiary palaeoeclimates. *Review of Palaeobotany and Palynology* 71: 149–190.

Grímsson, F., G. W. Grimm, R. Zetter, and T. Denk. 2016. Cretaceous and Paleogene Fagaceae from North America and Greenland: evidence from a Late Cretaceous split between Fagus and the remaining Fagaceae. *Acta Palaeobotanica* 56: 247–305.

Hagen, E. R., D. L. Royer, R. A. Moye, and K. R. Johnson. 2019. No large bias within species between the reconstructed areas of complete and fragmented fossil leaves. *Palaios* 34: 43–48.

Hennig, D., and L. Kunzmann. 2013. Taphonomy and vegetational analysis of a late Eocene flora from Schleenhain (Saxony, Germany). *Geologica Saxonica* 59: 75–88.

Hovenden, M. J., and J. K. Vander Schoor. 2003. Nature vs nurture in the leaf morphology of Southern beech, *Nothofagus cunninghamii* (Nothofagaceae). *New Phytologist* 161: 585–594.

Hren, M. T., N. D. Sheldon, S. T. Grimes, M. E. Collinson, J. J. Hooker, M. Bugler, and K. C. Lohmann. 2013. Terrestrial cooling in Northern Europe during the Eocene-Oligocene transition. *Proceedings of the National Academy of Sciences* 110: 7562–7567.

Knobloch, E., M. Konzalová, and Z. Kvaček. 1996. Die obereozäne Flora der Staré Sedlo-Schichtenfolge in Böhmen (Mitteleuropa). *Rozpravy Ústředního ústavu geologického* 49: 1–260.

Kriegel, K. 2001. Untersuchung der Blattmorphologie und Blattanatomie von *Eotrigonobalanus furcinervis* (Rossmäßler) Walther & Kvaček und seine Vergesellschaftung mit anderen teriären Sippen vom Mitteleozän bis Oligo-/Miozän Mitteleuropas. Diploma thesis, Technical University Dresden, Dresden, Germany.

Krutzsch, W. 2011. Stratigrafie und Klima des Palaogens im Mitteldeutschen Astuar im Vergleich zur marinen nordlichen Umrahmung. *Zeitschrift der Deutschen Gesellschaft für Geowissenschaften* 162: 19–47.

Kunzmann, L. 2012. Early Oligocene plant taphocoenosis with mass occurrence of *Zingiberoideophyllum* (extinct Zingiberales) from central Germany. *Palaios* 27: 765–778.

Kunzmann, L., Z. Kvaček, V. Teodoridis, Ch. Müller, and K. Moraweck. 2016. Vegetation dynamics of riparian forest in central Europe during the late Eocene. *Palaeontographica Abteilung B* 295: 67–88.

Kunzmann, L., D. Uhl, and P. S. Krüger. 2018. Whitish leaves in Eocene lignites in central Germany—a brief survey from the viewpoint of palaeobotany. *Freiberger Forschungshefte C* 554: 213–223.

Kvaček, Z. 2010. Forest flora and vegetation of the European early Palaeogene - a review. *Bulletin of Geosciences* 85: 63–76.

Kvaček, Z., and H. Walther. 1989a. Revision der mitteleuropaischen Fagaceen nach blattepidermalen Charakteristiken: Teil III. T. *Dryophyllum* Debey ex Saporta und *Eotrigonobalanus* Walther and Kvaček gen. nov. *Feddes Repertorium* 100: 575–601.

Kvaček, Z., and H. Walther. 1989b. Paleobotanical studies in Fagaceae of the European Tertiary. *Plant Systematics and Evolution* 162: 213–229.

Kvaček, Z., V. Teodoridis, K. Mach, T. Přikryl, and Z. Dvořák. 2014. Tracing the Eocene-Oligocene transition: A case study from North Bohemia. *Bulletin of Geosciences* 89: 21–66.

Little, S. A., S. W. Kembel, and P. Wilf. 2010. Paleotemperature Proxies from Leaf Fossils Reinterpreted in Light of Evolutionary History. *PLoS One* 5: e15161.

Mai, D. H. 1995. Tertiäre Vegetationsgeschichte Europas: Methoden und Ergebnisse. Gustav Fischer, Jena, Germany.

Mai, D. H., and H. Walther. 2000. Die Fundstellen eozäner Floren NWSachsens und des Bitterfelder Raumes. *Altenburger Naturwissenschaftlichen Forschungen* 33: 3–59.

McDonald, P. G., C. R. Fonseca, J. McC. Overton, and M. Westoby. 2003. Leaf-size divergence along rainfall and soil-nutrient gradients: is the method of size reduction common among clades? *Functional Ecology* 17: 50–57.

Merkhofer, L., P. Wilf, M. T. Haas, R. M. Kooyman, L. Sack, C. Scoffoni, and N. R. Cúneo. 2015. Resolving Australian analogs for an Eocene Patagonian paleorainforest using leaf size and floristics. *American Journal of Botany* 102: 1160–1173.

Moles, A. T., S. E. Perkins, S. W. Laffan, H. Flores-Moreno, M. Awasthy, M. L. Tindall, L. Sack, et al. 2014. Which is a better predictor of plant traits: temperature or precipitation? *Journal of Vegetation Science* 25: 1167–1180.

Moraweck, K., M. Grein, W. Konrad, J. Kovar-Eder, J. Kvaček, C. Neinhuis, A. Roth-Nebelsick, et al. 2019. Leaf traits of long-ranging Paleogene species and their relationship with depositional facies, climate and atmospheric CO_2 level. *Palaeontographica Abteilung B* 298: 93–172.

Moraweck, K., D. Uhl, and L. Kunzmann. 2015. Estimation of late Eocene (Bartonian–Priabonian) terrestrial palaeoclimate: contributions from megafloral assemblages from central Germany. *Palaeogeography, Palaeoclimatology, Palaeoecology* 433: 247–258.

Mosbrugger, V., T. Utescher, and D. L. Dilcher. 2005. Cenozoic continental climatic evolution of Central Europe. *PNAS* 102: 14964–14969.

Okajima, Y., H. Taneda, K. Noguchi, and I. Terashima. 2012. Optimum leaf size predicted by a novel leaf energy balance model incorporating dependencies of photosynthesis on light and temperature. *Ecological Research* 27: 333–346.

Parkhurst, D. F., and O. L. Loucks. 1972. Optimal Leaf Size in Relation to Environment. *Journal of Ecology* 60: 505–537.

Peppe, D. J., D. L. Royer, B. Cariglino, S. Y. Oliver, S. Newman, E. Leight, G. Enikolopov, et al. 2011. Sensitivity of leaf size and shape to climate: global patterns and paleoclimatic applications. *New Phytologist* 190: 724–739.

Price, C. A., S.-J. C. Knox, and T. J. Brodribb. 2013. The influence of branch order on optimal leaf vein geometries: Murray's Law and area preserving branching. *PloS One* 8: e85420.

RStudio Team. 2016. RStudio: Integrated Development for R. Boston, MA: RStudio, Inc. http://www.rstudio.com/

Reich, P. B., I. J. Wright, J. Cavender-Bares, J. M. Craine, J. Oleksyn, M. Westoby, and M. B. Walters. 2003. The evolution of plant functional variation: traits, spectra, and strategies. *International Journal of Plant Sciences* 164: 143–164.

Rossmässler, E. A. 1840. Die Versteinerungen des Braunkohlensandsteines aus der Gegend von Altsattel in Böhmen (Ellbogener Kreis). 42 pp. Arnoldsche Buchhandlung Dresden, Leipzig.

Roth-Nebelsick, A., M. Grein, C. Traiser, K. Moraweck, L. Kunzmann, J. Kovar-Eder, J. Kvaček, et al. 2017. Functional leaf traits and leaf economics in the Paleogene—A case study for Central Europe. *Palaeogeography, Palaeoclimatology, Palaeoecology* 472: 1–14.

Royer, D. L. 2012. Climate reconstruction from leaf size and shape: New developments and challenges. *The Paleontological Society Papers* 18: 195–212.

Royer, D. L., D. J. Peppe, E. A. Wheeler, and Ü. Niinemets. 2012. Roles of climate and functional traits in controlling toothed vs. untoothed leaf margins. *American Journal of Botany* 99: 915–922.

Royer, D. L., L. Sack, P. Wilf, C. H. Lusk, G. J. Jordan, Ü. Niinemets, I. J. Wright, et al. 2007. Fossil leaf economics quantified: Calibration, Eocene case study, and implications. *Paleobiology* 33: 574–589.

Rüffle, L., W. R. Muller Stoll, and R. Litke. 1976. Weitere Ranales, Fagaceae, Loranthaceae, Apocynaceae. In *Eozane Floren des Geiseltales*, Autorenkollektiv (eds). Abhandlungen des Zentralen Geologischen Instituts Berlin, Paläontologie-Abhandlungen 26, 199–282.

Sack, L., and C. Scoffoni. 2013. Leaf venation: structure, function, development, evolution, ecology and applications in the past, present and future. *New Phytologist* 198: 983–1000.

Sack, L., C. Scoffoni, A. D. McKow, K. Frole, M. Rawls, C. Havran, H. Tran, et al. 2012. Developmentally based scaling of the leaf venation architecture explains global ecological patterns. *Nature Communication* 3: 837.

Schneider, C. A., W. S. Rasband, and K. W. Eliceiri. 2012. NIH Image to ImageJ: 25 years of image analysis. *Nature Methods* 9: 671–675.

Scoffoni, C., M. Rawls, A. McKown, H. Cochard, and L. Sack. 2011. Decline of leaf hydraulic conductance with dehydration: relationship to leaf size and venation architecture. *Plant Physiology* 156: 832–843.

Standke, G., D. Escher, J. Fischer, and J. Rascher. 2008. Das Tertiär Nordwestsachsens: Ein geologischer Überblick. Sächsisches Landesamt für Umwelt, Landwirtschaft und Geologie, Freiberg, Germany.

Su, T., Y.-W. Xing, Y.-S. Liu, F. M. B. Jacques, W.-Y. Chen, Y.-J. Huang, and Z.-K. Zhou. 2010. Leaf Margin Analysis: A new equation from humid to mesic forests in China. *Palaios* 25: 234–238.

Tanrattana, M., A. Boura, F. M. B. Jacques, L. Villier, F. Fournier, A. Enguehard, S. Cardonnet, et al. 2020. Climatic evolution in Western Europe during the Cenozoic: Insights from historical collections using leaf physiognomy. *Geodiversitas* 42: 151–174.

Teodoridis, V., Z. Kvaček, H. Zhu, and P. Mazouch. 2012. Environmental analysis of the mid-latitudinal European Eocene sites of plant macrofossils and their possible analogues in East Asia. *Palaeogeography, Palaeoclimatology, Palaeoecology* 333–334: 40–58.

Tian, M., G. Yu, N. He, and J. Hou. 2016. Leaf morphological and anatomical traits from tropical to temperate coniferous forests: Mechanisms and influencing factors. *Scientific Reports* 6: 19703.

Traiser, C., S. Klotz, D. Uhl, and V. Mosbrugger. 2005. Environmental signals from leaves—a physiognomic analysis of European vegetation. *New Phytologist* 166: 465–484.

Traiser, C., A. Roth-Nebelsick, M. Grein, J. Kovar-Eder, L. Kunzmann, K. Moraweck, J. Lange, et al. 2018. MORPHYLL: A database of fossil leaves and their morphological traits. *Palaeontologia Electronica* 21: 1–17.

Traiser, C., A. Roth-Nebelsick, J. Lange, and J. Kovar-Eder. 2015. MORPYHLL—database for acquisition of ecophysiologically relevant morphometric data of fossil leaves. Version 1.0. State Museum of Natural History Stuttgart.

Uhl, D. 2006. Fossil plants as palaeoenvironmental proxies—some remarks on selected approaches. *Acta Palaeobotanica* 46: 87–100.

Uhl, D. 2014. Variability of selected leaf traits in European beech (*Fagus sylvatica*) in relation to climatic factors—some implications for palaeoenvironmental studies. *Phytologia Balcania* 20: 145–153.

Uhl, D., and V. Mosbrugger. 1999. Leaf venation density as a climate and environmental proxy: a critical review and new data. *Palaeogeography, Palaeoclimatology, Palaeoecology* 149: 15–26.

Uhl, D., H. Walther, and V. Mosbrugger. 2002. Leaf venation density in angiosperm leaves as related to climatic and environmental conditions-problems and potential for palaeoclimatology. *Neues Jahrbuch für Geologie und Paläontologie-Abhandlungen* 224: 49–95.

Violle, C., M.-L. Navas, D. Vile, E. Kazakou, C. Fortunel, I. Hummel, and E. Garnier. 2007. Let the concept of trait be functional! *Oikos* 116: 882–892.

Webb, L. J. 1959. A physiognomic classification of Australian rainforests. *The Journal of Ecology* 47: 551–570.

Westerhold, T., N. Marwan, A. J. Drury, D. Liebrand, C. Agnini, E. Anagnostou, J. S. K. Barnet, et al. 2020. An astronomically dated record of Earth's climate and its predictability over the last 66 million years. *Science* 369: 1383–1387.

Wilf, P. 1997. When are leaves good thermometers? A new case for Leaf Margin Analysis. *Paleobiology* 23: 373–390.

Winterscheid, H., and Z. Kvaček. 2016. Late Oligocene macrofloras from fluviatile siliciclastic facies of the Köln Formation at the south-eastern border of the Lower Rhine Embayment (North Rhine-Westphalia, Germany). *Acta Palaeobotanica* 56: 41–64.

Wolfe, J. A. 1979. Temperature parameters of humid to mesic forests of eastern Asia and relation to forests of other regions of the Northern Hemisphere and Australasia. *United States Geological Survey Professional Paper* 1106: 1–37.

Wolfe, J. A. 1993. A method of obtaining climatic parameters from leaf assemblages. *U.S. Geological Survey Bulletin*, Washington. 73 p.

Wolfe, J. A., and R. A. Spicer. 1999. Fossil Leaf Character States: Multivariate Analysis. *In* T. P. Jones and N. P. Rowe [eds.], Fossil Plants and Spores: Modern Techniques, 233–239, Geological Society London.

Wright, I. J., P. B. Reich, M. Westoby, D. D. Ackerly, Z. Baruch, F. Bongers, J. Cavender-Bares, et al. 2004. The worldwide leaf economics spectrum. *Nature* 428: 821–827.

Wright, I. J., N. Dong, V. Maire, I. C. Prentice, M. Westoby, S. Díaz, R. V. Gallagher, et al. 2017. Global climatic drivers of leaf size. *Science* 357: 917–921.

Yang, J., R. A. Spicer, T. E. V. Spicer, N. C. Arens, F. M. B. Jacques, T. Su, E. M. Kennedy, et al. 2015. Leaf form-climate relationships on the global stage: an ensemble of characters. *Global Ecology and Biogeography* 24: 1113–1125.

Yang, J., R. A. Spicer, T. E. V. Spicer, and C.-S. Li. 2011. 'CLAMP' Online: a new web-based palaeoclimate tool and its application to the terrestrial Paleogene and Neogene of North America. *Palaeobiodiversity and Palaeoenvironments* 91: 163–183.

Zachos, J. C., G. R. Dickens, and R. E. Zeebe. 2008. An early Cenozoic perspective on greenhouse warming and carbon-cycle dynamics. *Nature* 451: 279–283.

Zachos, J. C., M. Pagani, L. Sloan, E. Thomas, and K. Billups. 2001. Trends, rhythms, and aberrations in global climate 65 Ma to present. *Science* 292: 686–693.

Peppe, D. J., A. Baumgartner, A. Flynn, and B. Blonder. 2018. Reconstructing paleoclimate and paleoecology using fossil leaves. *In* D. A. Croft, D. F. Su, and S. W. Simpson [eds.], Methods in Paleoecology, 289–317. New York, NY: Springer International Publishing.